

The enterobactin biosynthetic intermediate 2,3-dihydroxybenzoic acid is a competitive inhibitor of the *Escherichia coli* isochorismatase EntB

Xue Bin | Peter D. Pawelek 

Department of Chemistry and Biochemistry,
Concordia University, Montreal, Quebec,
Canada

Correspondence

Peter D. Pawelek, Department of Chemistry
and Biochemistry, Concordia University, 7141
Sherbrooke St., W., Montreal, QC H4B 1R6,
Canada.

Email: peter.pawelek@concordia.ca

Funding information

Natural Sciences and Engineering Research
Council of Canada, Grant/Award Number:
341983

Review Editor: Lynn Kamerlin

Abstract

The *Escherichia coli* enterobactin biosynthetic protein EntB is a bifunctional enzyme that catalyzes hydrolysis of isochorismate via its N-terminal isochorismatase (IC) domain, and then transfers phosphopantetheinylated 2,3-DHB to EntF via the EntB C-terminal aryl carrier protein (ArCP) domain. Here we used a fluorescence anisotropy binding assay to investigate the ability of 2,3-DHB to bind to enzymes in the DHB synthetic arm of the pathway. We found that 2,3-DHB binds to EntE as a natural substrate with high affinity ($K_D = 0.54 \mu\text{M}$). Furthermore, *apo*-EntB was found to bind to 2,3-DHB with moderate affinity ($K_D = 8.95 \mu\text{M}$), despite the fact that this intermediate is neither a substrate nor a product of EntB. Molecular docking simulations predicted a top-ranked ensemble in which 2,3-DHB is bound at the isochorismatase active site of *apo*-EntB. Steady-state coupled enzymatic assays revealed that 2,3-DHB is a competitive inhibitor of *apo*-EntB isochorismatase activity ($K_i \sim 200 \mu\text{M}$), consistent with modeling predictions. Monitoring the EntC–EntB coupled reaction in real time via isothermal titration microcalorimetry confirmed that EntB was required to drive the EntC reaction toward isochorismate formation. Furthermore, addition of 2,3-DHB to the ITC-monitored reaction resulted in a suppression of integrated reaction heats, consistent with our observation that the molecule acts as a competitive inhibitor of EntB. Finally, we found that 2,3-DHB lowered the efficiency of EntC–EntB isochorismate channeling by approximately 70%, consistent with steric blockage of the isochorismatase active site by bound 2,3-DHB. Given its inhibitory properties, we hypothesize that 2,3-DHB plays a regulatory role in feedback inhibition in order to maintain iron homeostasis upon intracellular accumulation of sufficient ferric enterobactin.

KEYWORDS

enterobactin, enzyme inhibitor, enzyme kinetics, fluorescence anisotropy, isothermal titration calorimetry, molecular docking, protein–protein interaction, siderophore, site-directed mutagenesis

1 | INTRODUCTION

Siderophores are iron-chelating molecules secreted by numerous prokaryotic species as well as some

eukaryotes in order to scavenge scarce extracellular ferric iron under aerobic conditions (Neilands, 1995; Renshaw et al., 2002). Enterobactin is a catecholate siderophore with extraordinarily high affinity for ferric

This is an open access article under the terms of the [Creative Commons Attribution-NonCommercial-NoDerivs](https://creativecommons.org/licenses/by-nc-nd/4.0/) License, which permits use and distribution in any medium, provided the original work is properly cited, the use is non-commercial and no modifications or adaptations are made.

© 2025 The Author(s). *Protein Science* published by Wiley Periodicals LLC on behalf of The Protein Society.

iron ($K_D \sim 10^{-35}$ M at physiological pH) (Carrano & Raymond, 1979). It is comprised of three 2,3-dihydroxybenzoic acid (2,3-DHB) subunits connected via a triserine trilactone core. While 2,3-DHB itself has iron-chelating properties, the three-dimensional triscatechol arrangement of three DHB moieties in enterobactin confers optimal affinity for Fe^{3+} ($K_A = 10^{52} \text{ M}^{-1}$) (Harris et al., 1979; Raymond et al., 2003). In addition to being an enterobactin precursor, 2,3-DHB has also been reported to be a precursor for other siderophores (vibriobactin and anguibactin), and to function as a secondary metabolite in plants as a response to pathogen infection (Bartsch et al., 2010; Marín et al., 2012).

Since over-accumulation of iron leads to cellular damage, biosynthesis of enterobactin is tightly regulated (Buss et al., 2001). Expression of the genes encoding enterobactin biosynthetic enzymes (*entC*, *entB*, *entA*, *entE*, *entF*, *entD*, and *entH*) is controlled by the protein Ferric Uptake Regulator (Fur). In iron-replete conditions, *holo*-Fur binds to the promoters of three *ent* gene clusters, silencing gene expression. Upon iron starvation, *apo*-Fur dissociates from the promoters, resulting in up-regulation of *ent* gene products and subsequent enterobactin biosynthesis (Andrews et al., 2003; Brickman et al., 1990). In *Escherichia coli*, enterobactin is synthesized in the cytoplasm in two stages. In the first stage (Figure 1), the biosynthetic intermediate 2,3-DHB is produced from chorismate by sequential reactions catalyzed by three enzymes: (i) EntC (isochorismate synthase; EC 5.4.4.2), (ii) the N-terminal isochorismatase (IC) domain of EntB (EC 3.3.2.1), and (iii) EntA (2,3-dihydro-2,3-dihydroxybenzoate dehydrogenase; EC 1.3.1.28). In the second stage of the pathway, 2,3-DHB is adenylated by EntE (2,3-dihydroxybenzoyl-AMP ligase; EC 6.2.1.71) in an ATP-dependent reaction in order to

facilitate its covalent attachment to the aryl carrier protein (ArCP) domain of EntB and subsequent delivery to phosphopantetheinylated EntF (enterobactin synthase). Enterobactin production from activated 2,3-DHB then involves three EntF-catalyzed cycles of condensation with L-serine via the formation of non-ribosomal peptide bonds followed by cyclization and product release (Lai et al., 2006). Enterobactin is produced in the cytoplasm and secreted to the extracellular environment by a TolC-dependent process (Corinna et al., 2005). Following secretion, enterobactin chelates extracellular ferric iron, and the ferric-enterobactin complex is then imported via TonB-dependent uptake (Raymond et al., 2003).

In order to deliver 2,3-DHB to *holo*-EntF, the ArCP domain of *apo*-EntB itself must be phosphopantetheinylated at Ser 245 by the accessory enzyme EntD to form *holo*-EntB. The catalytic efficiency of phosphopantetheinylation at the EntB C-terminal domain is insensitive to the presence of the N-terminal IC domain (Gehring et al., 1997). Similarly, the N-terminal isochorismatase activity of EntB has been shown to be insensitive to the phosphopantetheinylation status of the C-terminal ArCP domain (Jiang & Guo, 2007). In agreement with these observations, our group has reported that enterobactin biosynthesis and secretion can still occur in an *E. coli entB*[−] knockout strain transformed with two expression constructs under Fur control that encoded discrete functional IC and ArCP domains (Pakarian & Pawelek, 2016).

The bifunctional nature of EntB, as well as its promiscuity in forming pairwise interactions with other enzymes in the pathway (EntC, EntA, EntE, EntF, Drake et al., 2006; Khalil & Pawelek, 2009; Lai et al., 2006; Ouellette et al., 2022; Pakarian & Pawelek, 2016) highlights the central role EntB plays in enterobactin biosynthesis. We consider EntB to be a

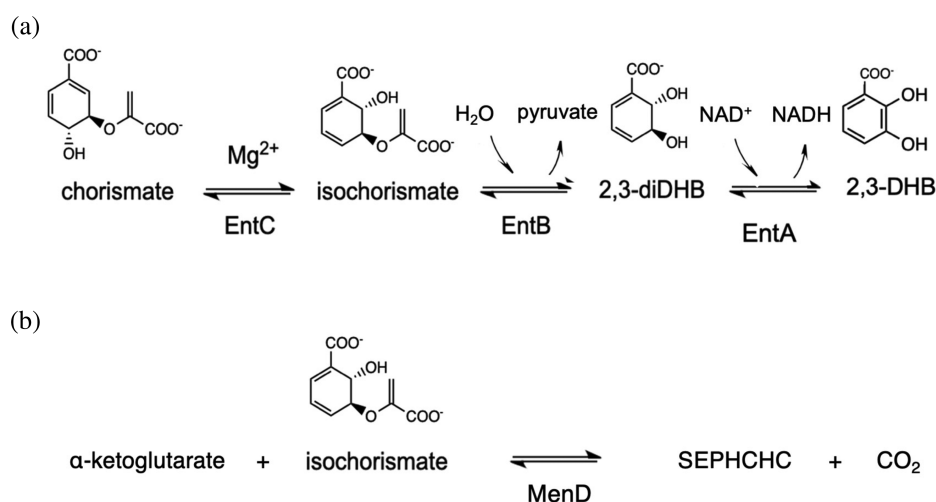


FIGURE 1 Reaction scheme. (a) Reactions catalyzed by EntB, EntC, and EntA. (b) Reaction catalyzed by MenD. SEPHCHC: 2-succinyl-5-enolpyruvyl-6-hydroxy-3-cyclohexene-1-carboxylate.

protein–protein interaction (PPI) hub, playing not only a catalytic role but also a structural role in promoting the formation of a biosynthetic multienzyme complex similar to the pyoverdine siderosome reported in *Pseudomonas aeruginosa* (Imperi & Visca, 2013). In support of this, we have produced in vivo crosslinking results demonstrating that EntC, EntB, EntA, and EntE co-migrate as a cross-linked species isolated from iron-depleted *E. coli* cell lysates (unpublished data). We have also recently reported evidence of leaky isochorismate channeling between EntC and EntB in vitro (Bin & Pawelek, 2024), demonstrating that pairwise PPIs between Ent enzymes can function to optimize metabolite flux in the direction of 2,3-DHB formation.

Given the central role played in enterobactin biosynthesis, EntB is a likely target for regulation. In living organisms, accumulation of intracellular iron is toxic due to the Fenton reaction and production of reactive oxygen species leading to cell death (Dixon & Stockwell, 2014). Regulation of enterobactin biosynthesis in *E. coli* is essential for maintaining iron homeostasis, especially following attainment of sufficient intracellular iron. It has long been known, for example, that in an iron-rich environment the genes necessary for enterobactin biosynthesis are repressed by *holo*-Fur (Lucía et al., 1999). However, beyond Fur repression, our current understanding of how enterobactin biosynthesis is regulated is highly limited. Here we report novel evidence of competitive inhibition of EntB by 2,3-DHB, which is neither a substrate nor a product of this enzyme. Given such an inhibitory role, we hypothesize that 2,3-DHB can additionally serve as a negative feedback regulator of iron homeostasis.

2 | MATERIALS AND METHODS

2.1 | Reagents

2,3-DHB, porcine lactate dehydrogenase (LDH) and chorismic acid were purchased from Sigma-Aldrich (St. Louis, MO). All other reagents were purchased from Bioshop Canada, Inc. (Burlington, ON).

2.2 | Molecular docking and analysis

Atomic coordinates of 2,3-DHB (ligand) and the dimeric EntB x-ray crystallographic structure (receptor) were obtained from Protein Data Bank (PDB ID: DBH (Berman et al., 2000) and 2FQ1 (Drake et al., 2006), respectively). Polar hydrogens were added and Kollman charges were assigned using MGLTools (v1.5.7) (Sanner, 1999). Blind docking was performed with Achilles Blind Docking server (Bioinformatics and High Performance Computing (BIO-HPC) Research group, n.d.), in which the whole EntB surface was made

available for ligand search. Restrained docking was performed with AutoDock Vina (v1.1.2) (Eberhardt et al., 2021; Trott & Olson, 2010), in which the surface of the EntB isochorismatase was interrogated for possible DHB binding sites. Conformers with the lowest binding energy from each method were selected for docking analysis using PyMOL (Schrodinger LLC, 2015). The EntB monomer (PDB ID: 2FQ1, chain A (Drake et al., 2006)) was submitted to ConSurf database (Ben Chorin et al., 2020; Goldenberg et al., 2009) for identifying the conservation of ligand-interacting residues.

2.3 | Protein expression and purification

Protein overexpression and purification were performed as reported previously (Bin & Pawelek, 2024) following transformation of expression constructs into competent AG-1 cells following established protocols (Sambrook & Russell, 2006). Briefly, constructs containing in-frame N-terminal hexahistidine tagged EntB (WT and variants) and MenD harboring pCA24N plasmids (ASKA repository (Kitagawa et al., 2005)) were transformed into *E. coli* AG-1 cells. Constructs containing in-frame N-terminal hexahistidine tagged EntC harboring pET24b plasmid were transformed into *E. coli* BL21(DE3) cells. Cells were grown in LB (or 2xYT for EntC) broth containing 30 µg/mL chloramphenicol (or kanamycin for EntC) at 37 °C to a final OD₆₀₀ between 0.6 and 0.8. Overexpression of recombinant proteins was induced by 0.5 mM isopropyl β-D-1-thiogalactopyranoside (IPTG) overnight at 16–22°C.

Cells were lysed by ultrasonic homogenizer (Biologics) in a buffer containing 50 mM HEPES (pH 8.0), 500 mM NaCl, 5% glycerol, 10 mM imidazole, 2 mM β-mercaptoethanol, and protease inhibitor cocktail. Cell lysate was centrifuged for 1.5 h at 47,850g, and the supernatant was collected. Clarified lysate was applied to a metal ion affinity column (Profinity IMAC resin, Bio-Rad Laboratories) connected to a BioLogic DuoFlow FPLC system (Bio-Rad Laboratories). Target proteins were eluted using a linear gradient of imidazole (10–400 mM imidazole) in a buffer containing 50 mM HEPES (pH 8.0), 500 mM NaCl, 5% glycerol, and 2 mM β-mercaptoethanol. Pooled fractions containing purified proteins were dialyzed against 50 mM HEPES (pH 8.0), 150 mM NaCl, 1.0 mM tris(2-carboxyethyl)phosphine (TCEP) and 15% glycerol. Dialyzed samples were stored at –20°C. Protein concentrations were determined by measuring absorbance at 280 nm and using molar extinction coefficients predicted from primary amino acid sequences ($\epsilon = 51,910 \text{ M}^{-1} \text{ cm}^{-1}$, $31,970 \text{ M}^{-1} \text{ cm}^{-1}$ and $107,285 \text{ M}^{-1} \text{ cm}^{-1}$ for EntB, EntC and MenD, respectively) (Gasteiger et al., 2005).

2.4 | Fluorescence anisotropy

Reaction mixtures containing 2 μM of 2,3-DHB and varying concentrations of protein in Assay Buffer (50 mM HEPES (pH 8.0), 150 mM NaCl and 1 mM TCEP) were preincubated at room temperature for 10 min. Fluorescence measurements ($\lambda_{\text{ex}} = 315 \text{ nm}$, $\lambda_{\text{em}} = 437 \text{ nm}$; slit width: 10 nm) were carried out at 21°C on Varian Cary Eclipse spectrofluorometer using a 10 mm pathlength quartz cuvette (Hellma). Fluorescence anisotropy (γ) was calculated using equation $\gamma = \frac{I_{VV} - G \times I_{VH}}{I_{VV} + 2 \times G \times I_{VH}}$, where I_{VV} and I_{VH} represent fluorescence intensities obtained vertically polarized excitation (V in italic subscript) and vertically or horizontally polarized emission (V or H in italic subscript, respectively); G is an instrument-dependent correction factor. Apparent binding affinity (K_D) values were determined by fitting the data to the one-site total binding model (GraphPad Prism): $Y = \frac{B_{\text{max}} \times X}{K_D + X} + \text{NS} \times X + \text{BG}$, where Y represents the binding signal, X represents ligand concentration, B_{max} represents maximal specific binding, NS represents nonspecific binding, BG represents background, and K_D represents the equilibrium dissociation constant.

2.5 | EntB isochorismatase activity assay

Enzymological assays were carried out at 21°C using a Genesys 10 Spectrophotometer. Due to the lack of commercial availability of isochorismate, we prepared an equilibrium mixture of chorismate:isochorismate as reported previously (Bin & Pawelek, 2024) by incubating 256 or 1026 μM chorismate with 0.50 μM EntC in Assay Buffer containing 5 mM MgCl_2 in an ice bath for 20 min, which was expected to yield a chorismate:isochorismate ratio of approximately 3:2 (Hubrich et al., 2014). Once the reaction reached equilibrium, the chorismate:isochorismate mixture was isolated by centrifugation at 10,000g for 7 min through a 0.5 mL centrifugal filter (3K MWCO, Pall Corporation). Chorismate:isochorismate mixtures were freshly prepared on the day of use.

Reaction mixtures containing 0.10 μM EntB, 1.50 unit/mL LDH, and 350 μM NADH in Assay Buffer were preincubated at room temperature for 10 minutes. Enzymatic reactions were initiated by the addition of the chorismate:isochorismate equilibrium mixture to a final concentration range between 6.2 and 73.9 μM . Reactions were followed by measuring the decrease in NADH absorbance at 340 nm. Initial velocities were calculated by linear fitting of OD₃₄₀ decrease using the VISIONlite Rate software (Thermo Scientific). Fits of data to steady-state enzyme kinetic models was performed using Kaleidagraph (Synergy Software).

Steady-state kinetic assays of EntB isochorismatase were performed in the presence of 0, 100, 250 and 400 μM of 2,3-DHB. Kinetics data were fit to the Michaelis–Menten model to determine K_m and V_{max} values. In order to further characterize 2,3-DHB inhibition behavior, Eadie–Hofstee plots of steady-state kinetics data were generated using Kaleidagraph, and K_i values were determined by a linear replot of slope values at specific 2,3-DHB concentrations.

2.6 | Substrate channeling: MenD competition assay

Kinetic assays of EntC–EntB–LDH coupled reactions were carried out using similar conditions as for the EntB–LDH coupled assay above. Excess MenD was added to the reaction mixtures (final concentration: 6.25 μM) in Assay Buffer containing 0.05 μM EntC, 1.25 μM EntB, 50 μM thiamine pyrophosphate, and 660 μM 2-ketoglutarate (the latter two reagents being MenD co-substrates) in the presence of 0.35 mM 2,3-DHB. The reactions were initiated by the addition of chorismate to a final concentration of 26 μM . Initial velocities were calculated by linear regression fitting of observed OD₃₄₀ decrease using the VISIONlite Rate software (Thermo Scientific). After correction for background, isochorismatase activity in the presence of excess MenD was divided by that in the absence of MenD in order to calculate the efficiency of substrate channeling (expressed as a percentage).

2.7 | Isothermal titration microcalorimetry

All ITC measurements were performed on a VP-ITC Microcalorimeter (Microcal, Inc.). To monitor the coupled EntC–EntB enzymatic reaction by ITC, enzymes were diluted in ITC Buffer (50 mM HEPES (pH 8.0), 150 mM NaCl, 1 mM TCEP, 10 mM MgCl_2), extensively degassed, and transferred into the instrument's sample cell. The instrument syringe contained 79 μM chorismate in ITC buffer. ITC experiments were performed at a constant temperature of 30°C. Each experiment involved two syringe injections of 30 μL over a 60-s interval with constant stirring at 300 RPM, and with a 10-min spacing time between the injections. EntC was added to the sample cell at a final concentration of 313 nM in the absence or presence of EntB (wild-type or variant as appropriate) (concentration range: 162–2587 nM). Integrated reaction heats were quantitated using Microcal Origin (Microcal, Inc.). Integrated heats of enzymatic reactions were corrected for the heat of injection (30 μL ITC buffer injected into ITC buffer), as well as the heat of dilution of chorismate into ITC buffer minus protein.

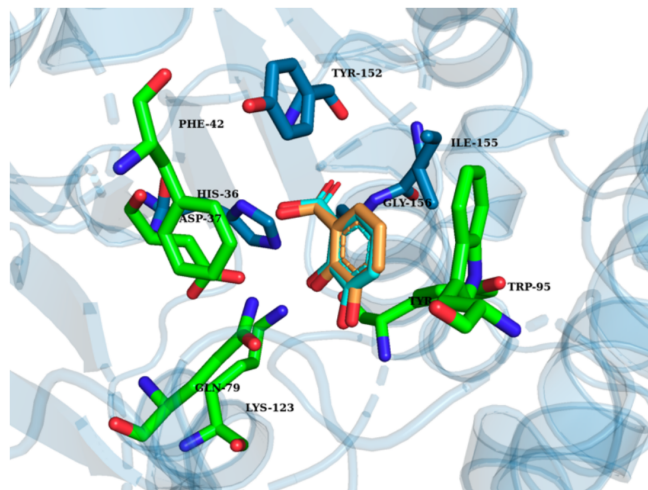


FIGURE 2 Automated docking simulation of EntB binding to 2,3-DHB. EntB shown in cartoon presentation (helices = coils; strands = arrows); ligand (2,3-DHB) and EntB residues in contact with ligand are shown as sticks with carbon atoms colored as follows: Green = EntB catalytic residues; dark blue = EntB residues in contact with bound ligand; orange = the top-ranked DHB binding pose from blind docking; cyan = top-ranked DHB binding pose from restrained docking (RMSD = 0.009 Å).

3 | RESULTS AND DISCUSSION

Our initial observation of 2,3-DHB interaction with *E. coli* EntB arose from a broader study we performed in which we investigated the ability of various DHB isomers to quench intrinsic fluorescence of EntB and EntE, and found that 2,3-DHB was able to specifically quench EntB fluorescence unlike 3,5-DHB and 2,5-DHB (Khalil & Pawelek, 2009). Given our recent finding that EntC and EntB interact (Ouellette et al., 2022) to form a dynamic channeling system (Bin & Pawelek, 2024), we decided to revisit and expand on this observation to see if 2,3-DHB might also play a functional role in the EntCB coupled reaction.

3.1 | Computational modeling of 2,3-DHB binding at the EntB active site

To identify possible 2,3-binding sites on the surface of EntB, we performed automated docking experiments, taking both a blind docking approach as well as a restrained docking approach. The blind docking simulation using 2,3-DHB as a ligand and dimeric EntB as a receptor produced 24 energetically favorable docked ensembles. The ensembles were ranked by the binding energy, which ranged from -7.0 to -3.6 kcal/mol. The most energetically favorable pose of 2,3-DHB was located at the active site of EntB (Figure 2). Moreover, residues involved in the predicted EntB-DHB interaction overlapped with six out of 10 residues reported by Drake et al. (2006) as being catalytically important. In

addition to blind docking simulations, a restrained docking simulation was performed that produced nine energetically favorable models (binding energy range: -6.9 to -6.0 kcal/mol); the pose of the top-ranked model from the restrained docking approach was superimposable with the pose of the top-ranked model from the blind docking approach (RMSD = 0.009 Å) (Figure 2, cyan and orange binding poses).

3.2 | Equilibrium-binding of 2,3-DHB to EntB: Fluorescence anisotropy

We previously reported the binding of DHB isomers to EntB via fluorescence spectroscopy, in which the EntB intrinsic fluorescence was found to be most strongly quenched by 2,3-DHB in comparison with other DHB analogues (2,5-dihydroxybenzoic acid (2,5-DHB) and 3,5-dihydroxybenzoic acid (3,5-DHB)) (Khalil & Pawelek, 2009). Since 2,3-DHB is fluorescent ($\lambda_{\text{ex}} = 315$ nm, $\lambda_{\text{em}} = 437$ nm), here we measured changes in 2,3-DHB fluorescence anisotropy to better understand equilibrium-binding characteristics of 2,3-DHB when interacting with relevant target proteins (Figure 3). We found that 2,3-DHB bound to EntE with relatively high affinity (apparent $K_D = 0.54$ μM), consistent with 2,3-DHB being a natural substrate of EntE (Figure 3a). We further found that 2,3-DHB binds specifically to EntB, exhibiting binding behavior consistent with the single-site binding model (apparent $K_D = 8.95$ μM) (Figure 3b). Additionally, we previously reported (Bin & Pawelek, 2024) that EntB residue R196 is essential for isochorismate channeling between EntC and EntB as well as electrostatically guiding isochorismate to the EntB active site. Fluorescence anisotropy experiments further revealed that 2,3-DHB binds to the EntB variant R196A with much lower affinity than wild-type EntB (Figure 3c; apparent K_D not determinable due to insufficient approach to saturation). The lowered affinity of 2,3-DHB for this variant, previously shown to be deficient in EntCB isochorismatase channeling, is consistent with our previous observation that EntB R196 is also involved in electrostatically guiding isochorismate to the isochorismatase active site (Bin & Pawelek, 2024).

3.3 | EntB isochorismatase: Steady-state kinetics

EntB isochorismatase activity was measured in a coupled assay with excess LDH as reported previously (Bin & Pawelek, 2024). In this assay, isochorismate is converted to 2,3-dihydro-2,3-dihydroxybenzoate (2,3-diDHB) and pyruvate by EntB isochorismatase activity; LDH-catalyzed conversion of pyruvate to lactate is then monitored by loss of OD₃₄₀ following

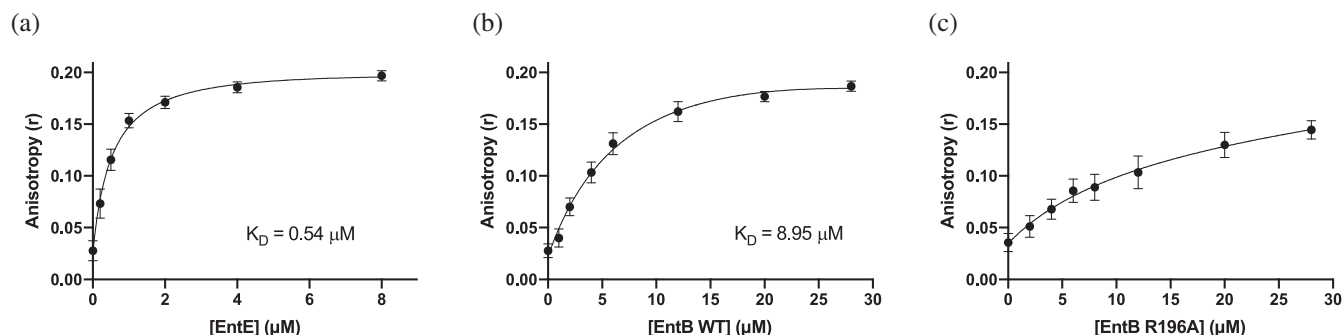


FIGURE 3 Fluorescence anisotropy binding assays. (a) EntE, (b) wild-type EntB, (c) EntB R196A. In all cases, purified protein was titrated into 2.00 μM of 2,3-DHB and fluorescence anisotropy was measured at each protein concentration ($\lambda_{\text{ex}} = 315 \text{ nm}$, $\lambda_{\text{em}} = 437 \text{ nm}$). Data are shown as the mean of triplicate independent measurements; error bars represent standard deviations from the mean. Apparent K_D values determined from fits of the data to the single-site binding model; apparent K_D for 2,3-DHB binding to EntB R196A not determinable due to insufficient approach to saturation over concentration range.

TABLE 1 Steady-state kinetic parameters of wild-type EntB isochorismatase in the absence and presence of 2,3-DHB.

[2,3-DHB] (μM)	Isochorismate apparent K_m (μM)	V_{max} ($\mu\text{M min}^{-1}$)
0	9.21 ± 0.97	4.91 ± 0.22
100	16.24 ± 1.57	5.25 ± 0.17
250	22.12 ± 3.25	4.99 ± 0.52
400	32.55 ± 0.23	5.33 ± 0.05

Note: Enzyme kinetics data were obtained using the EntB-LDH coupled enzyme assay (0.1 μM EntB) initiated with a 3:2 equilibrium mixture of chorismate and isochorismate.

oxidation of NADH to NAD^+ . The Hill coefficient from an IC_{50} dose–response curve of EntB isochorismatase inhibition by 2,3-DHB was 1.16 (Figure S1), consistent with a DHB:EntB binding stoichiometry of 1.0 (Prinz, 2010). Coupled assay kinetics data for the conversion of isochorismate to 2,3-diDHB were fit to the Michaelis–Menten steady-state kinetics model, resulting in an apparent Michaelis–Menten constant ($K_{m, \text{app}}$) equal to 9.2 μM (Table 1, Row 2, Column 2), which is similar to a published K_m value for EntB isochorismatase ($K_m = 14.7 \mu\text{M}$), as determined using a different experimental approach (Rusnak et al., 1990). Given this similarity, we concluded that our coupled assay was suitable for investigating possible inhibition of EntB isochorismatase activity by 2,3-DHB in the absence of EntC.

3.4 | Inhibition of EntB isochorismatase by 2,3-DHB

We performed a series of steady-state kinetic assays in which EntC, EntB, and LDH activities were coupled (Bin & Pawelek, 2024) to investigate the effect of increasing concentrations of 2,3-DHB on overall coupled enzyme activity. Our kinetics data showed that

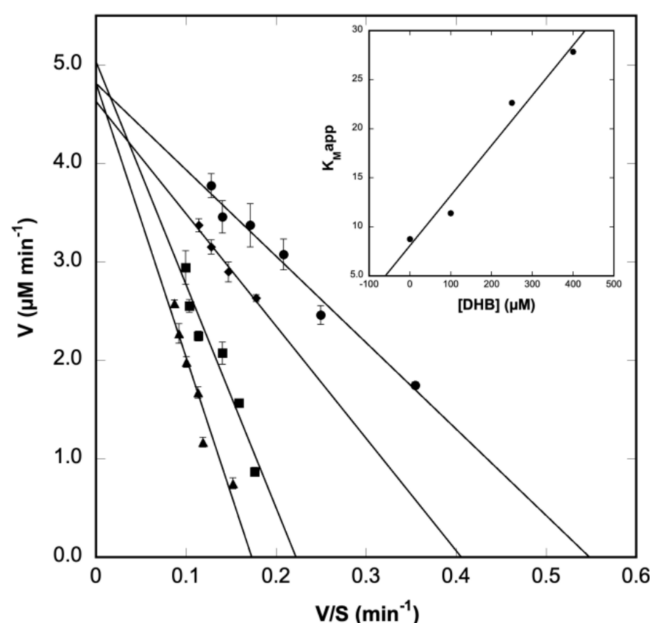


FIGURE 4 Eadie–Hofstee plot of EntB-LDH coupled assay kinetics in the presence and absence of 2,3-DHB. Circles: 0 μM 2,3-DHB, diamonds: 100 μM 2,3-DHB, squares: 250 μM 2,3-DHB, triangles: 400 μM 2,3-DHB. Data shown with the mean and standard deviation of triplicate independent measurements. Inset: Replot of linear slope values as a function of 2,3-DHB concentration. The K_i value was determined from the slope of the linear replot.

the EntB K_m value for isochorismate decreased as a function of 2,3-DHB concentration (Table 1, Column 2), whereas V_{max} values were unaffected by the presence of 2,3-DHB (Table 1, column 3). Kinetics data were further analyzed using an Eadie–Hofstee plot. Linear fits of the data were observed to approximately converge at the ordinate, indicative of competitive inhibition (Figure 4). A replot of the slopes obtained from the Eadie–Hofstee linear fits (i.e., the apparent K_m values for isochorismate) as a function of DHB concentration resulted in an apparent K_i value of 200 μM (Figure 4,

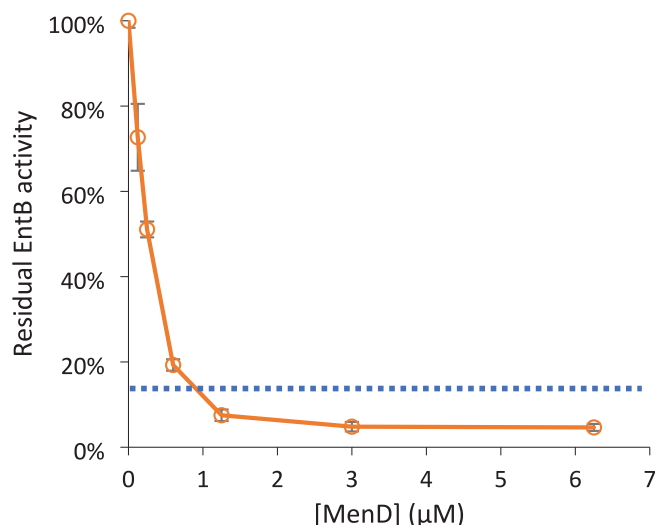


FIGURE 5 The effect of 2,3-DHB on the EntC–EntB isochorismate channeling. Residual EntB Activity = EntB isochorismate activity in the presence of 350 μ M 2,3-DHB and MenD (0–6.25 μ M). Data were measured in triplicate. Standard deviations from the mean are indicated with error bars. Dashed line indicates 16% EntC–EntB isochorismate channeling measured previously reported (Imperi & Visca, 2013) under identical conditions but in the absence of 2,3-DHB.

inset). This K_i value is similar to the intracellular concentration of 2,3-DHB in exponentially growing *E. coli* cells (~ 140 μ M) (Bennett et al., 2009), supporting a biological role for 2,3-DHB in the inhibition of EntB isochorismatase.

We previously reported partial channeling of isochorismate in an EntC–EntB–LDH coupled assay in which approximately 16% residual isochorismatase activity was observed in the presence of a competing isochorismate-utilizing enzyme, MenD (Bin & Pawelek, 2024). Here, we repeated our channeling experiment, but in the presence of 2,3-DHB. Residual EntB isochorismatase activity in the presence of excess MenD, a measure of substrate channeling efficiency, was observed to decrease to approximately 5% in the presence of 2,3-DHB (Figure 5), reflecting an overall 70% decrease in isochorismate channeling efficiency in the presence of 350 μ M 2,3-DHB. Consistent with our competitive inhibition data, we conclude that 2,3-DHB binds at the active site of EntB isochorismatase, and in doing so obstructs the continuous channeling surface between EntC and EntB active sites (Bin & Pawelek, 2024).

3.5 | ITC measurements of EntC–EntB reaction and inhibition by DHB

Isothermal titration microcalorimetry is a technique in which heat evolved or absorbed by a reaction is measured, allowing for calculation of thermodynamic

parameters (ΔG , ΔH , ΔS). Typically, ITC is used for studying binding reactions given its utility in determining K_D and stoichiometry values of a particular binding system. In addition, ITC has been successfully used to follow steady-state enzyme kinetics (Siddiqui et al., 2022; Wang et al., 2020). We, therefore, decided to employ ITC to follow the EntC–EntB coupled reaction in real time without the need for a coupled reporter enzyme like LDH. We performed recurrent single-injection assays (Wang et al., 2020) in which the EntC substrate (chorismate) was injected into a sample cell containing dilute EntC with or without EntB. Two injections of 79 μ M chorismate into a sample cell containing 313 nM EntC in ITC buffer resulted in very low heat evolution compared with a control injection lacking chorismate, suggesting that the EntC-catalyzed isomerization of chorismate to isochorismate has a relatively low enthalpy change. Repetition of the experiment, but with the addition of EntB to the sample cell, resulted in a large increase in heat evolution in a manner dependent on the concentration of added EntB (Figure 6a). The rapid return to baseline as a function of EntB concentration for each injection supports our prior report of EntC–EntB substrate channeling (Bin & Pawelek, 2024). Given the complexity of the EntC–EntB coupled reaction (i.e., dynamic channeling following EntC–EntB pairwise interaction, each having its own heat signature in addition to those of the intrinsic EntC and EntB enzymatic reactions), deconvolution of observed heats into discrete kinetic rate constants was not possible. However, integration of thermal spikes following chorismate injection allowed for relative comparison of EntCB activity as a function of increasing EntB concentration (Figure 6b). Overall heat evolution was observed to rapidly increase up to an EntB:EntC molar ratio of 1:1, followed by a more gradual increase going from 2:1 to 8:1 EntB:EntC. The observed gradual increase is likely due to approach to saturation of EntCB complex formation at higher EntB concentrations, since dynamic channeling requires transient interaction of EntC and EntB (Bin & Pawelek, 2024). We also performed the EntC–EntB ITC experiment in the absence of Mg^{2+} . In this case, only the heat of injection was observed, confirming that the observed heats were indeed due to magnesium-dependent EntC enzymatic activity (Figure 6c). Furthermore, it has previously been reported that the EntC-catalyzed reaction is highly reversible (Liu et al., 1990), and that EntB may assist in metabolic flux in the direction of 2,3-DHB formation by rapidly converting isochorismate to 2,3-diDHB thus preventing its EntC-catalyzed conversion back to chorismate. Our ITC results support these observations. Since we could use ITC to interrogate the effect of EntB on the EntC reaction, we also investigated the effect of 2,3-DHB addition to the sample cell while EntB was present. We found that heat evolution decreased in a DHB-dependent manner (Figure 6d)

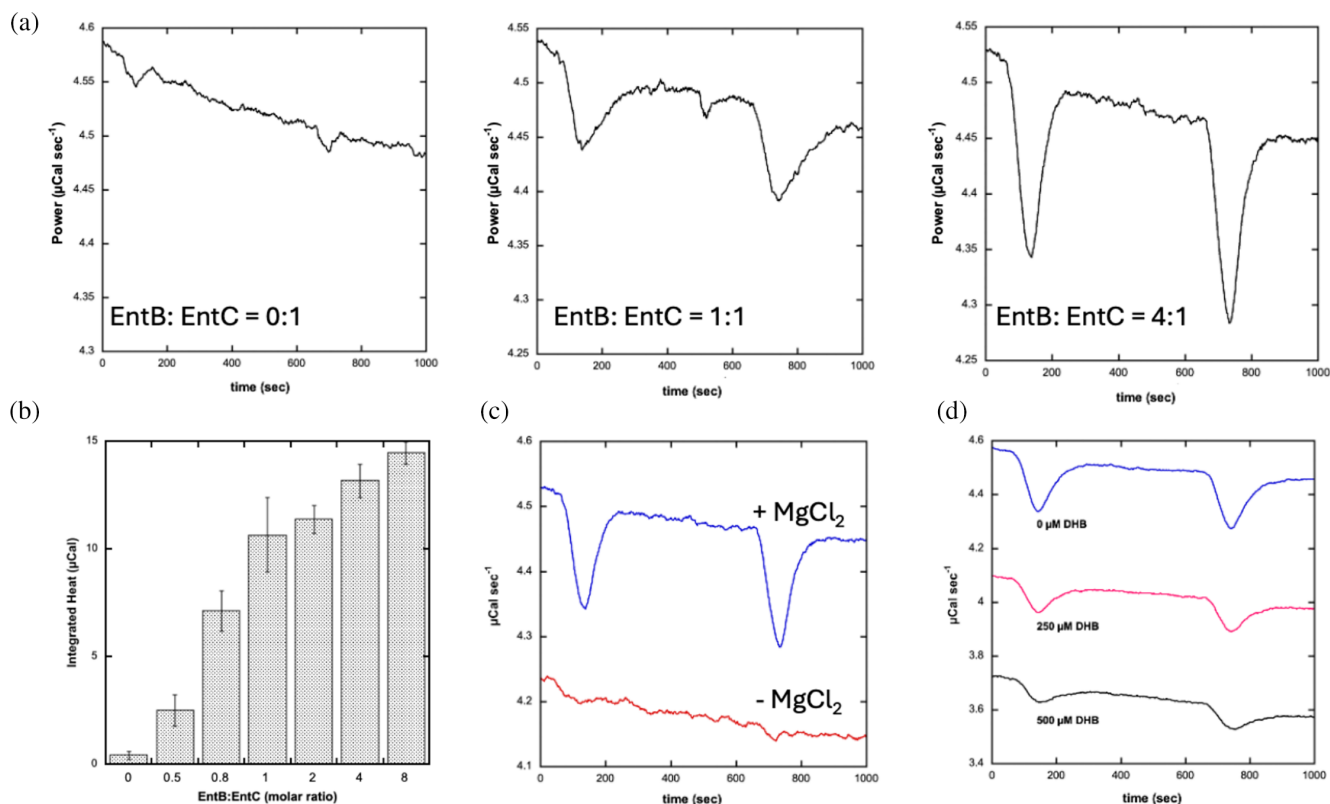


FIGURE 6 Isothermal titration microcalorimetry of the EntC-catalyzed reaction. (a) Recurrent single-injection assays of EntC enzymatic activity in the absence and presence of EntB. Raw thermograms showing heats evolved upon injection of chorismate into a reference cell containing 313 nM EntC and increasing concentrations of EntB (left panel: 0 nM EntB, middle panel: 323 nM EntB, right panel: 1293 nM EntB). All panels rendered to the same scale. (b) Corrected integrated heats of the EntC-catalyzed reaction as a function of EntB concentration. (c) Raw thermograms showing magnesium dependence of the EntB-driven EntC reaction (313 nM EntC, 1293 nM EntB): Blue: 10 mM MgCl_2 , red: 0 mM MgCl_2 + 10 mM EDTA. Thermograms arbitrarily offset along the ordinate for the purpose of comparison. (d) Raw thermograms showing the effect of 2,3-DHB on the EntB-driven EntC reaction (313 nM EntC, 1293 nM EntB): Blue: 0 μM DHB, red: 250 μM DHB, black: 500 μM DHB. Thermograms arbitrarily offset along the ordinate for the purpose of comparison.

consistent with our analysis of EntCB steady-state kinetics data in which the competitive inhibition of EntB by 2,3-DHB was found to have an apparent K_i value of approximately 200 μM .

4 | CONCLUSIONS

Although several chorismate analogs have been reported to inhibit EntB isochorismatase activity (Hubrich et al., 2013; Rusnak et al., 1990), this study presents the first evidence that 2,3-DHB can function as a competitive inhibitor of EntB isochorismatase. To further explore the nature of 2,3-DHB binding to EntB, which we had first observed as 2,3-DHB-dependent quenching of intrinsic EntB fluorescence (Khalil & Pawelek, 2009), we employed automated docking simulations and equilibrium-binding experiments. Both molecular docking simulations and steady-state enzyme kinetics studies demonstrated that 2,3-DHB is a competitive inhibitor of EntB isochorismatase. Furthermore, ITC experiments revealed that the rate of

conversion of chorismate to 2,3-diDHB increased in an EntB-dependent manner, supporting our previous observation of EntCB channeling of isochorismate. Taken together, these *in vitro* observations suggest that 2,3-DHB may play a biological role as a negative feedback regulator of enterobactin biosynthesis via direct inhibition of EntB following accumulation of sufficient intracellular iron. Given the highly reversible nature of EntC activity, inhibition of EntB isochorismatase therefore would target the committed step of the enterobactin biosynthetic pathway. Disruption of isochorismate channeling by 2,3-DHB would result in non-productive diffusion of the labile intermediate into the bulk cytosol or re-routing to other metabolic fates. Similar feedback regulation has also been found in the enzyme complex that catalyzes the first two sequential reactions of tryptophan biosynthesis in *E. coli*, anthranilate synthetase (TrpE) and phosphoribosyl transferase (TrpD), where tryptophan acts on TrpE while cooperatively inhibiting TrpD in its complex formed with TrpE. On the other hand, the regulation of TrpE is allosteric inhibition instead of competitive inhibition (Naz et al., 2023; Pabst

et al., 1973). Given the promiscuity of EntB binding to other enzymes in the enterobactin biosynthetic pathway (EntC, EntA, EntE, and EntF), we are now interested in understanding this interplay between biosynthesis and its regulation in the context of larger multienzyme assemblies (i.e., EntCBAE). Moreover, these results reveal that EntB may serve as an excellent target for disruption of enterobactin-mediated iron uptake in a therapeutic context.

AUTHOR CONTRIBUTIONS

Xue Bin: Investigation; writing – original draft; methodology; validation; visualization; writing – review and editing. **Peter D. Pawelek:** Conceptualization; investigation; funding acquisition; writing – original draft; methodology; validation; visualization; writing – review and editing; supervision; resources.


ACKNOWLEDGMENTS

This work was supported by Discovery Grant 341983 from the Natural Sciences and Engineering Research Council of Canada to P.D. Pawelek. Additional financial support for X. Bin was provided by J.W. McConnell Memorial Doctoral Fellowship. We thank Dr. Eric Brown at McMaster University for providing the *menD* ASKA strain used in this study.

DATA AVAILABILITY STATEMENT

The data that support the findings of this study are available from the corresponding author upon reasonable request.

ORCID

Peter D. Pawelek  <https://orcid.org/0000-0002-8361-6593>

REFERENCES

- Andrews SC, Robinson AK, Rodríguez-Quiriones F. Bacterial iron homeostasis. *FEMS Microbiol Rev*. 2003;27(2–3):215–37.
- Bartsch M, Bednarek P, Vivancos PD, Schneider B, von Roepenack-Lahaye E, Foyer CH, et al. Accumulation of isochorismate-derived 2,3-dihydroxybenzoic 3-O-β-D-xyloside in Arabidopsis resistance to pathogens and ageing of leaves. *J Biol Chem*. 2010;285(33):25654–65.
- Ben Chorin A, Masrati G, Kessel A, et al. ConSurf-DB: an accessible repository for the evolutionary conservation patterns of the majority of PDB proteins. *Protein Sci*. 2020;29(1):258–67. <https://doi.org/10.1002/pro.3779>
- Bennett BD, Kimball EH, Gao M, Osterhout R, van Dien SJ, Rabinowitz JD. Absolute metabolite concentrations and implied enzyme active site occupancy in *Escherichia coli*. *Nat Chem Biol*. 2009;5(8):593–9.
- Berman HM, Westbrook J, Feng Z, et al. The protein data bank. *Nucl Acids Res*. 2000;28(1):235–42.
- Bin X, Pawelek PD. Evidence of isochorismate channeling between the *Escherichia coli* enterobactin biosynthetic enzymes EntC and EntB. *Protein Sci*. 2024;33(8):e5122.
- Bioinformatics and High Performance Computing (BIO-HPC) Research group. Achilles Blind Docking Server. Available: <https://bio-hpc.ucam.edu/achilles/>
- Brickman TJ, Ozenberger BA, McIntosh MA. Regulation of divergent transcription from the iron-responsive fepB-entC promoter-operator regions in *Escherichia coli*. *J Mol Biol*. 1990;212(4):669–82.
- Buss K, Müller R, Dahm C, Gaitatzis N, Skrzypczak-Pietraszek E, Lohmann S, et al. Clustering of isochorismate synthase genes *menF* and *entC* and channeling of isochorismate in *Escherichia coli*. *Biochim Biophys Acta—Gene Struct Expr*. 2001;1522(3):151–7.
- Carrano CJ, Raymond KN. Ferric ion sequestering agents. 2. Kinetics and mechanism of iron removal from transferrin by enterobactin and synthetic tricatechols. *J Am Chem Soc*. 1979;101(18):5401–4.
- Corinna B, Cornelia G, Nadine T, et al. TolC is involved in Enterobactin efflux across the outer membrane of *Escherichia coli*. *J Bacteriol*. 2005;187(19):6701–7.
- Dixon SJ, Stockwell BR. The role of iron and reactive oxygen species in cell death. *Nat Chem Biol*. 2014;10(1):9–17.
- Drake EJ, Nicolai DA, Gulick AM. Structure of the EntB multidomain nonribosomal peptide synthetase and functional analysis of its interaction with the EntE adenylation domain. *Chem Biol*. 2006;13(4):409–19.
- Eberhardt J, Santos-Martins D, Tillack AF, Forli S. AutoDock Vina 1.2.0: new docking methods, expanded force field, and python bindings. *J Chem Inf Model*. 2021;61(8):3891–8.
- Gasteiger E, Hoogland C, Gattiker A, et al. Protein identification and analysis tools on the ExPASy server BT. In: Walker JM, editor. *The proteomics protocols handbook*. Totowa, NJ: Humana Press; 2005. p. 571–607.
- Gehring AM, Bradley KA, Walsh CT. Enterobactin biosynthesis in *Escherichia coli*: isochorismate lyase (EntB) is a bifunctional enzyme that is phosphopantetheinylated by EntD and then acylated by EntE using ATP and 2,3-dihydroxybenzoate. *Biochemistry*. 1997;36(28):8495–503.
- Goldenberg O, Erez E, Nimrod G, Ben-Tal N. The ConSurf-DB: pre-calculated evolutionary conservation profiles of protein structures. *Nucleic Acids Res*. 2009;37 Database issue:D323–7.
- Harris WR, Carrano CJ, Raymond KN. Spectrophotometric determination of the proton-dependent stability constant of ferric enterobactin. *J Am Chem Soc*. 1979;101:2213–4.
- Hubrich F, Mordhorst S, Andexer JN. Cinnamic acid derivatives as inhibitors for chorismatases and isochorismatases. *Bioorg Med Chem Lett*. 2013;23(5):1477–81.
- Hubrich F, Müller M, Andexer JN. In vitro production and purification of isochorismate using a two-enzyme cascade. *J Biotechnol*. 2014;191:93–8.
- Imperi F, Visca P. Subcellular localization of the pyoverdine biogenesis machinery of *Pseudomonas aeruginosa*: a membrane-associated “siderosome”. *FEBS Lett*. 2013;587(21):3387–91.
- Jiang M, Guo Z. Effects of macromolecular crowding on the intrinsic catalytic efficiency and structure of Enterobactin-specific Isochorismate synthase. *J Am Chem Soc*. 2007;129(4):730–1.
- Khalil S, Pawelek PD. Ligand-induced conformational rearrangements promote interaction between the *Escherichia coli* Enterobactin biosynthetic proteins EntE and EntB. *J Mol Biol*. 2009;393(3):658–71.
- Kitagawa M, Ara T, Arifuzzaman M, et al. Complete set of ORF clones of *Escherichia coli* ASKA library (a complete set of E. Coli K-12 ORF archive): unique resources for biological research. *DNA Res*. 2005;12(5):291–9. <https://doi.org/10.1093/dnares/dsi012>
- Lai JR, Fischbach MA, Liu DR, Walsh CT. A protein interaction surface in nonribosomal peptide synthesis mapped by combinatorial mutagenesis and selection. *Proc Natl Acad Sci USA*. 2006;103(14):5314–9.
- Liu J, Quinn N, Berchtold GA, Walsh CT. Overexpression, purification, and characterization of isochorismate synthase (EntC), the first enzyme involved in the biosynthesis of enterobactin from chorismate. *Biochemistry*. 1990;29(6):1417–25.
- Lucía E, Jose P-M, Víctor de L. Opening the iron box: transcriptional metallorepression by the fur protein. *J Bacteriol*. 1999;181(20):6223–9.

- Marín M, Plumeier I, Pieper DH. Degradation of 2,3-Dihydroxybenzoate by a novel *meta*-cleavage pathway. *J Bacteriol*. 2012;194(15):3851–60.
- Naz S, Liu P, Farooq U, Ma H. Insight into de-regulation of amino acid feedback inhibition: a focus on structure analysis method. *Microb Cell Fact*. 2023;22(1):161.
- Neilands JB. Siderophores: structure and function of microbial iron transport compounds (*). *J Biol Chem*. 1995;270(45):26723–6.
- Ouellette S, Pakarian P, Bin X, Pawelek PD. Evidence of an intracellular interaction between the *Escherichia coli* enzymes EntC and EntB and identification of a potential electrostatic channeling surface. *Biochimie*. 2022;202:159–65.
- Pabst MJ, Kuhn JC, Somerville RL. Feedback regulation in the anthranilate aggregate from wild type and mutant strains of *Escherichia coli*. *J Biol Chem*. 1973;248(3):901–14.
- Pakarian P, Pawelek PD. Intracellular co-localization of the *Escherichia coli* enterobactin biosynthetic enzymes EntA, EntB, and EntE. *Biochem Biophys Res Commun*. 2016;478(1):25–32.
- Prinz H. Hill coefficients, dose-response curves and allosteric mechanisms. *J Chem Biol*. 2010;3(1):37–44.
- Raymond KN, Dertz EA, Kim SS. Enterobactin: an archetype for microbial iron transport. *Proc Natl Acad Sci*. 2003;100:3584–8.
- Renshaw JC, Robson GD, Trinci APJ, Wiebe MG, Livens FR, Collison D, et al. Fungal siderophores: structures, functions and applications. *Mycol Res*. 2002;106(10):1123–42.
- Rusnak F, Liu J, Quinn N, Berchtold GA, Walsh CT. Subcloning of the enterobactin biosynthetic gene entB: expression, purification, characterization, and substrate specificity of isochorismatase. *Biochemistry*. 1990;29(6):1425–35.
- Sambrook J, Russell DW. Preparation and transformation of competent *E. coli* using calcium chloride. *Cold Spring Harb Protoc*. 2006;2006(1):pdb.prot3932.
- Sanner MF. Python: a programming language for software integration and development. *J Mol Graph Model*. 1999;17(1):57–61.
- Schrodinger LLC. The PyMOL Molecular Graphics System, v1.7.4.5 Edu Enhanced for Mac OS X. 2015.
- Siddiqui KS, Poljak A, Ertan H, Bridge W. The use of isothermal titration calorimetry for the assay of enzyme activity: application in higher education practical classes. *Biochem Mol Biol Educ*. 2022;50(5):519–26.
- Trott O, Olson AJ. AutoDock Vina: improving the speed and accuracy of docking with a new scoring function, efficient optimization, and multithreading. *J Comput Chem*. 2010;31(2):455–61. <https://doi.org/10.1002/jcc.21334>
- Wang Y, Wang G, Moitessier N, Mittermaier AK. Enzyme kinetics by isothermal titration calorimetry: Allosteric, inhibition, and dynamics. *Front Mol Biosci*. 2020;7:583826.

SUPPORTING INFORMATION

Additional supporting information can be found online in the Supporting Information section at the end of this article.

How to cite this article: Bin X, Pawelek PD. The enterobactin biosynthetic intermediate 2,3-dihydroxybenzoic acid is a competitive inhibitor of the *Escherichia coli* isochorismatase EntB. *Protein Science*. 2025;34(6):e70160. <https://doi.org/10.1002/pro.70160>